ELSEVIER

Catalysis Today 25 (1995) 241–247

CATALYSIS TODAY

Amorphous Pd–Si alloys for hydrogen-permeable and catalytically active membranes

Naotsugu Itoh [a,*], Takuya Machida [a], Wei-Chun Xu [a], Hisamichi Kimura [b], Tsuyoshi Masumoto [b]

[a] *National Institute of Materials and Chemical Research, 1-1 Higashi, Tsukuba 305, Japan*
[b] *Institute for Materials Research, Tohoku University, Sendai 980, Japan*

Abstract

Amorphous Pd_xSi_{1-x}(x=0.8, 0.825, 0.85) in the form of ribbon was prepared by a single-roller melt spinning technique to examine hydrogen permeability and catalytic activity for dehydrogenation. As a result, it was found that the amorphous specimens had higher tenacity and higher permeability of hydrogen than its crystallized form. Also, the surface of the amorphous specimen showed a catalytic activity for dehydrogenation of cyclohexane, while no activity was observed in the untreated. Taking advantage of both hydrogen permeability and catalytic activity, the amorphous Pd_xSi_{1-x} would be expected to be a candidate for a catalytic membrane.

1. Introduction

Amorphous alloys are well known to have interesting characteristics like high magnetic permeability, high corrosion resistance, high tenacity and so on. Furthermore, the disordered structure has been expected to affect the solubility and diffusivity of gas in the alloys very much. Many investigations on the solubility and diffusivity of hydrogen in amorphous Pd–Si alloys have been made [1–7]. Most of these studies, however, were carried out only at temperatures lower than 100°C since determination of the solubility and diffusivity were made exclusively by the electrochemical techniques, in which the upper temperature possible for measurements is limited because of using an aqueous solution. Furthermore, hydrogen permeability through amorphous alloys in gas phase has never been measured.

Therefore, the hydrogen permeability at high temperatures is required to determine in terms of applying the amorphous ribbon to a high-temperature hydrogen separation membrane for palladium membrane reactors [8]. In addition, since being not a simple function of solubility and diffusivity, the hydrogen permeability is necessary to be directly measured. On the other hand, several studies noting catalytic activity of amorphous alloys for methanation [9], olefin hydrogenation [10] and cyclohexene hydrogenation [11] have been made. Especially, effects of pre-treating amorphous alloys by oxidation on catalytic activity were intensively discussed.

In this study, both hydrogen permeability and catalytic activity for dehydrogenation of amorphous Pd–Si alloys will be examined at comparatively high temperature to inquire a possibility of

* Corresponding author.

SSDI 0920-5861(95)00121-2

applying those as hydrogen-permeable and/or catalytic membranes.

2. Experimental

2.1. Preparation of amorphous Pd–Si alloys

The amorphous Pd_xSi_{1-x} alloys with various compositions ($x=0.85$, 0.825, 0.80) used in the present study were prepared by rapid quenching from the melts using a single roller [12], which was made of copper and had a diameter of 300 mm and a width of 20 mm. The ribbon samples obtained had a mean thickness of about 40 μm and ca. 5 mm in width. Amorphous state of these samples was confirmed by X-ray analysis and differential scanning calorimetry (DSC).

2.2. Measurement of hydrogen permeability

Hydrogen permeation rate through the amorphous ribbon was measured using a permeation cell shown in Fig. 1. The effective area of membrane for permeation was 64 mm^2 (32 mm long $\times$ 2 mm wide). The membrane was clamped into the cell using aluminum foil as gas seal. The permeation experiments were carried out at a temperature ranging from 50 to 300°C and a hydrogen pressure ranging from 1 to 2 atm. After the temperature was raised to the desired value in argon, pure hydrogen of about 30 cc/min was introduced into hydrogen stream side, whereas into the other side the sweep gas (argon) at ambient pressure was made to flow at a flow rate of about 15 cc/min. Permeation tests at a heating rate of 1°C/min were also carried out to observe the process of crystallization. The pressures on the two sides of the membranes, the flow rates of effluent at outlet of permeation side, and cell temperature were recorded. The amount of permeated hydrogen was determined by gas chromatography.

2.3. Measurement of hydrogen solubility

A schematic diagram of an apparatus for hydrogen solubility measurement is shown in Fig. 2. The determining system consists of two cells: one is used as the standard, and the other is used as measuring cell. The sample was put into the measuring cell and the system was vacuumed. The sample cell was then heated to a desired temperature in an oil bath and kept overnight. Hydrogen gas was introduced into the standard cell at a certain pressure, where the moles introduced can be calculated by using the temperature T1 and pressure P1, as well as the cell volume. Next, the stop valve, V2, was opened and hydrogen was introduced into the sample cell. When the pressures were almost stable, the valve V2 was closed. The pressure P2 continually decreased as the hydrogen was absorbed by the sample. After the decrease in pressure P2 stopped, the moles of hydrogen remained in the standard and sample cells were calculated again from T1, T2, T3, P1, P2 and the cell volumes. The difference in the moles thus corresponded to the amount of hydrogen absorbed by sample. The hydrogen solubility in the amorphous

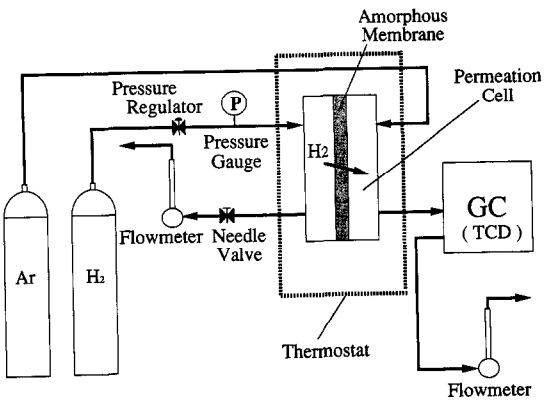

Fig. 1. Apparatus for measuring hydrogen permeation.

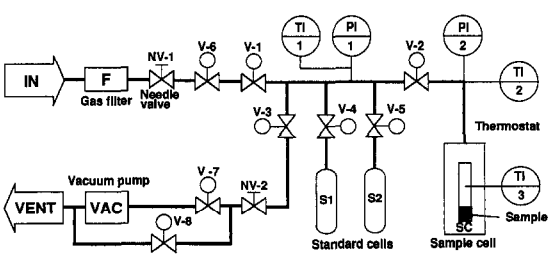

Fig. 2. Schematic diagram of the apparatus measuring hydrogen solubility.

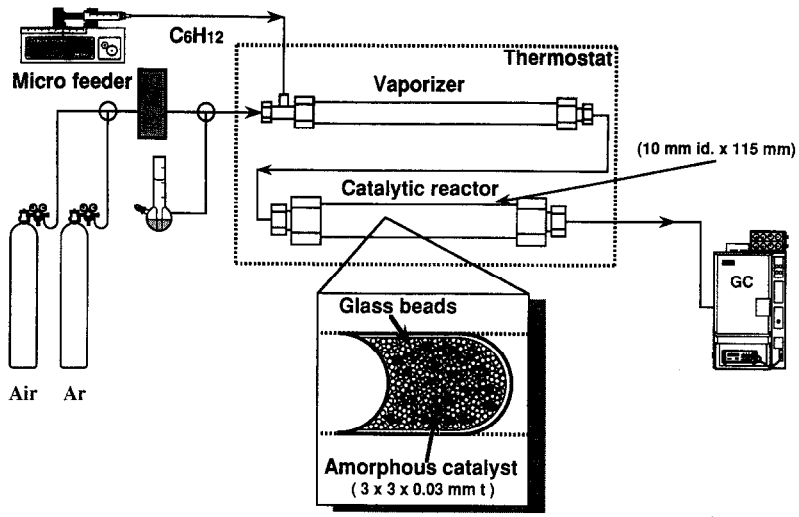

Fig. 3. Schematic diagram of the apparatus testing catalytic activity.

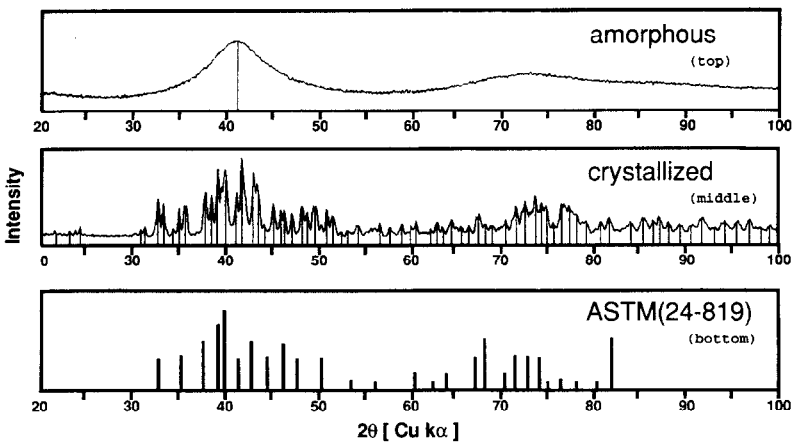

Fig. 4. XRD patterns of amorphous and crystallized $Pd_{0.8}Si_{0.2}$ alloy.

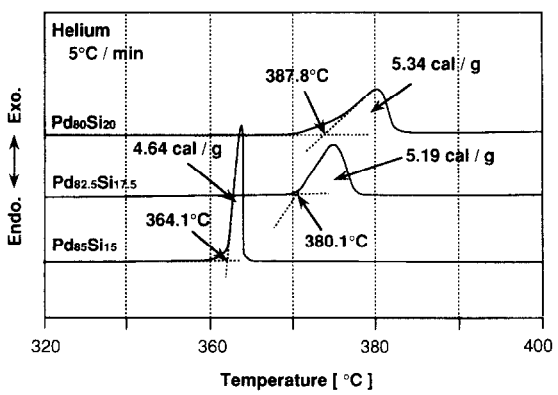

Fig. 5. DSC charts of Pd–Si alloys.

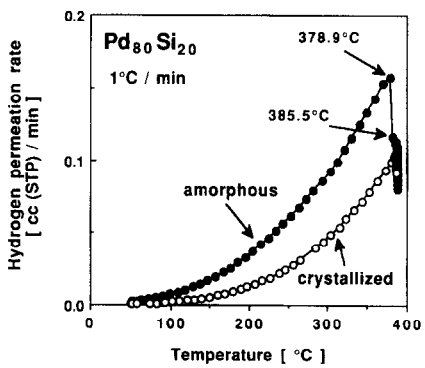

Fig. 6. Changes of the hydrogen permeation rate when heating at 1°C/min.

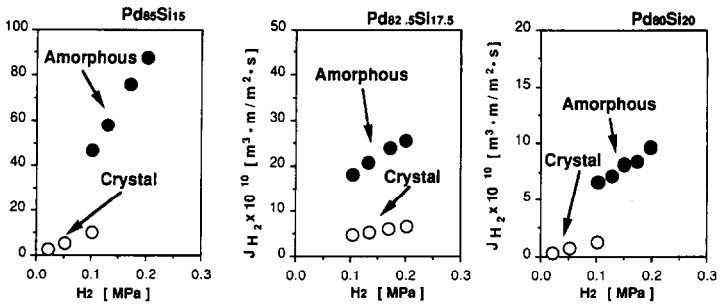

Fig. 7. Comparison of hydrogen permeability between amorphous and crystallized Pd_xSi_{1-x} at 473 K.

and crystallized alloys was measured in the range 50–200°C and 0.1–10 atm of hydrogen.

2.4. Dehydrogenation activity

A schematic diagram of an apparatus testing dehydrogenation activity is shown in Fig. 3. Dehydrogenation of cyclohexane to benzene was carried out under atmospheric pressure at temperatures of 423, 493 and 498 K. Cyclohexane was supplied by a micro-feeder at a constant flow rate (1.3 mg/min) and diluted to 4.5% with argon (8.2 cc (STP)/min) in a vaporizer and then sent to the flow reactor. In this study, $Pd_{0.8}Si_{0.2}$ amorphous ribbon of 3.09 g was used. Strips of ca. 3 mm × 3 mm cut from the ribbon together with glass beads (1.8 mm in average diameter) within the reactor tube (10 mm in inner diameter and 115 mm long) were uniformly packed. The degree of conversion was determined with gas chromatography with an FID detector.

Air treatment, that is, oxidation of the amorphous strips by air, was carried out at the reaction temperature for 60 min to examine changes in the dehydrogenation activity. The flow rate of dry air was 9.0 cc (STP)/min.

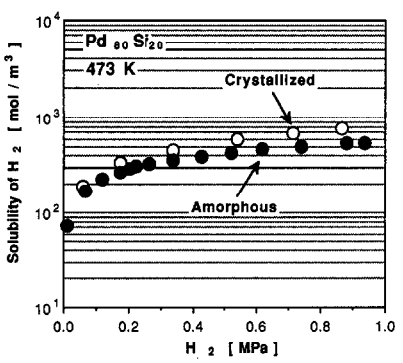

Fig. 8. Comparison of solubility between amorphous and crystallized ribbons.

3. Results and discussion

3.1. Confirmation of amorphous state

The X-ray diffraction pattern of all amorphous alloys showed a broad peak characteristic to the disordered structure as shown in Fig. 4 (top). DSC charts for three amorphous samples at a heating rate of 5°C/min in He are presented in Fig. 5. Exothermic heat due to crystallization can be seen for all the samples. The peak temperatures of crystallization in helium flow for different samples were found to be 364.1°C ($x=0.85$), 380.1°C ($x=0.825$), 387.8 ($x=0.80$)°C, respectively. A same result was obtained in hydrogen flow.

The crystallized one, for instance, $Pd_{0.80}Si_{0.20}$ alloy, shows sharp peaks in the XRD pattern as seen in Fig. 4 (middle). Although most of the peaks can be identified to be attributed to the $Pd_{0.8}Si_{0.2}$ alloy (Fig. 4, bottom), it is true that there remain some uncertain peaks. To clarify those peaks crystallographically further intensive study will be needed.

3.2. Hydrogen permeability and solubility

Fig. 6 shows change of the hydrogen permeability through the $Pd_{0.80}Si_{0.20}$ amorphous alloy at a heating rate of 1°C/min. The permeability was low at low temperatures, and increased rapidly with increasing temperature. However, the permeability sharply decreased when the temperature

Table 1
Measured densities of amorphous and crystallized $Pd_xSi_{(1-x)}$ alloys

	10.79 g / cm³	10.56 g / cm³	10.45 g / cm³
	11.06 g / cm³	10.73 g / cm³	10.60 g / cm³
	+2.5 %	+1.61 %	+1.44 %

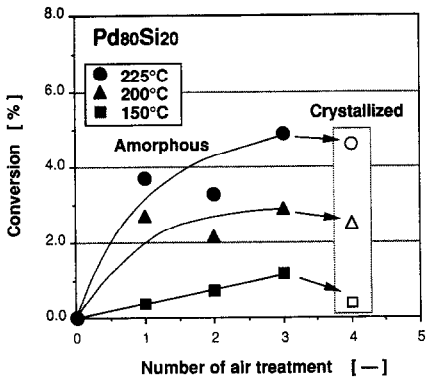

Fig. 9. Changes of catalytic activity due to air treatment.

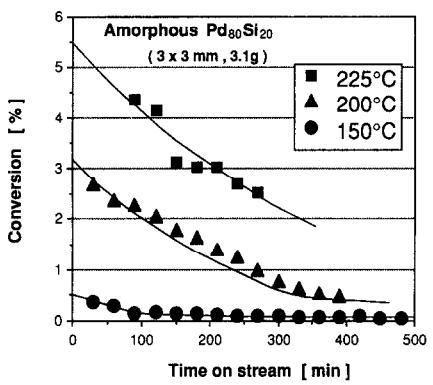

Fig. 10. Temporal changes of catalytic activity of amorphous strips after air treatment.

reached 379°C. This decrease was caused by the crystallization of the amorphous alloy, and continued until the crystallization completed. The permeability of the corresponding crystallized alloy was also determined and also plotted in Fig. 6. One can see that the permeability increases with temperature but is very low compared with that of amorphous one. Similarly, the permeabilities of hydrogen at 473 K for both the amorphous and its crystallized ribbons of the three alloys were compared in Fig. 7. Thus, it can be found that the crystallization of the amorphous alloys results in a large decrease of the hydrogen permeability.

Fig. 8 shows a comparison of the hydrogen solubility between amorphous and crystallized $Pd_{0.80}Si_{0.20}$ at 473 K. It is obvious that the crystallized ribbon has a little higher solubility than the amorphous, whereas in the case of $Pd_{0.825}Si_{0.175}$ and $Pd_{0.85}Si_{0.15}$ the amorphous ribbons have higher solubility than the crystallized. This fact seems to be strange considering that the amorphous ribbon has a higher permeability as was mentioned above. In general, the permeability of gas is given as a product of solubility and diffu-

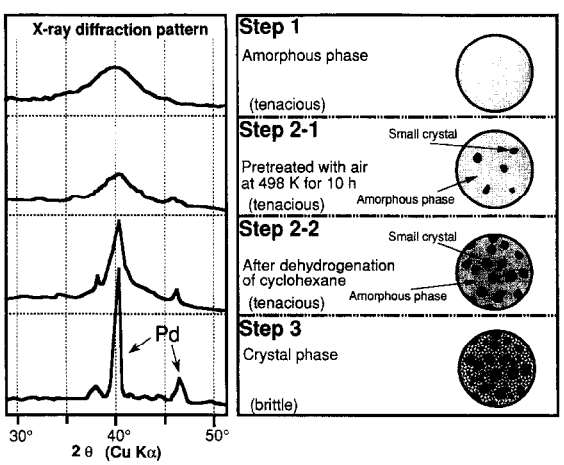

Fig. 11. XRD patterns and corresponding surface structure modeled.

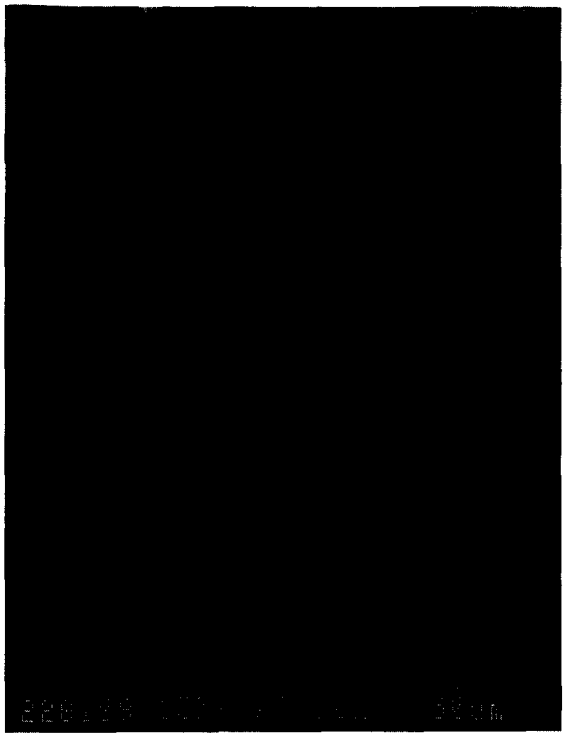

Fig. 12. A SEM image for the surface of crystallized $Pd_{0.8}Si_{0.2}$ ribbon used in the dehydrogenation run.

sivity. Therefore, it will be natural to think that the amorphous $Pd_{0.80}Si_{0.20}$ has a higher diffusivity. As one of the reasons to explain this phenomenon, densities of the three kinds of amorphous and the corresponding crystallized samples were determined according to the Archimedes principle. From the result shown in Table 1, it is clear that all the amorphous samples have lower densities than the crystallized. This means that there is more interstitial space available for hydrogen diffusion in the amorphous ribbons.

3.3. Catalytic activity

The effect of air treatment on the catalytic activity of amorphous $Pd_{0.8}Si_{0.2}$ was found to be very significant because the catalytic activity without air treatment was extremely low. However, a sudden increase of the activity was observed by the first treatment by air as seen in Fig. 9, where the cyclohexane conversions employed were obtained by extrapolation to the time of zero since the catalytic activity decreases with time as shown in Fig. 10. Such a decrease is considered to be caused by deactivation of the catalytic surface, which is probably covered by small palladium-rich crystallines as discussed below.

Further treatments led to a gradual increase in the initial activity, that is, rose in conversion. Such a drastic change is considered to be due to a change of surface structure of the amorphous alloy. Fig. 11 shows the X-ray diffraction patterns for the virgin amorphous, the air-treated and the crystallized ribbons. Simultaneously, a model illustrated the corresponding surface structure is shown. At steps 2–1 and 2–2 it is presumed from the XRD pattern, where a small peak specific for crystalline palladium near 40° appears, that fine palladium crystals are scatteringly grown in the

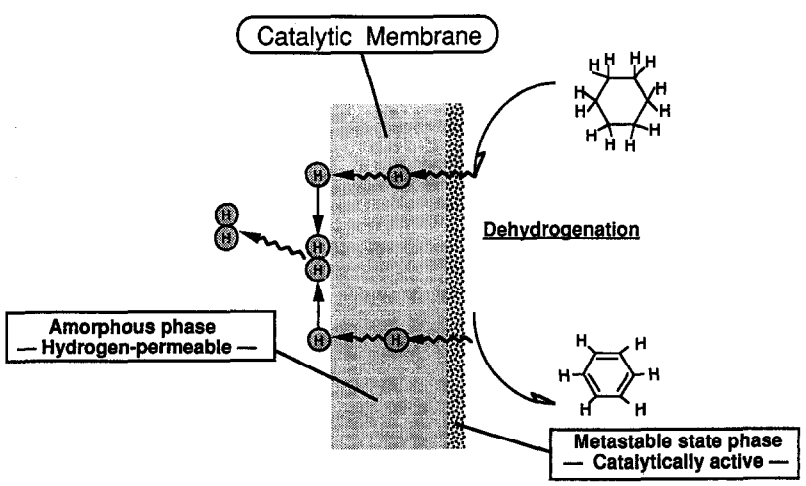

Fig. 13. A catalytic membrane system utilizing an amorphous alloy membrane.

bulk of amorphous state. A SEM photo at step 3 is shown in Fig. 12. This photo indicates that the growth of fine palladium-rich crystal particle results in the catalytic activity. In addition, the fact that the activity after the third treatment is similar to that of the crystallized as understood from Fig. 9 seems to support the above model.

3.4. Possibility of amorphous Pd–Si alloy as a catalytic membrane

It was made clear from the above discussion that the Pd–Si amorphous alloy has both the hydrogen permeability and the catalytic activity for dehydrogenation. Taking advantage of such two functions, a catalytic membrane system as depicted in Fig. 13 would be realized. One side of the amorphous membrane is only treated by air to make the catalytic activity emerge. This can make the bulk of the membrane maintain an amorphous structure and thereby a tenacity, which is easily lost by crystallization. A reaction scheme under consideration is that a dehydrogenation is carried out on the air-treated side, and the evolved hydrogen can be instantaneously removed to the other side through the amorphous membrane. The reverse scheme, of course, is possible, that is, hydrogen can be supplied from the left-hand side to the treated side, on which a hydrogenation of olefins, naphtens and so on can take place.

4. Conclusion

Amorphous Pd_xSi_{1-x} alloy ribbons were prepared by a single-roller melt spinning technique as one of rapid quenching methods to develop a new tenacious hydrogen-permeable membrane as well as a catalytic membrane. The hydrogen permeability, solubility and catalytic activity were examined.

It became clear that the hydrogen permeability of the amorphous ribbon has not only much larger hydrogen permeability but also much higher tenacity than the corresponding crystallized one. The crystallized was so brittle that one could not employ it as a membrane any longer.

Dehydrogenation runs of cyclohexane to benzene were carried out to examine the catalytic activity of an amorphous $Pd_{0.8}Si_{0.2}$ ribbon. Although the catalytic activity was extremely low before air treatment, it suddenly increased by the first air treatment, and was improved by further treatments. This was inferred to be due to a growth of fine palladium crystals in the surface of the ribbon by the air-treatment. At last, a catalytic membrane system was proposed by making use of both the hydrogen permeability and the catalytic activity.

References

[1] S. Filipek and B. Baranowski, J. Less-Common Metals, 89 (1983) 205.
[2] S.M. Filiper and A.W. Szafranski, J. Less-Common Metals, 101 (1984) 299.
[3] U. Stolz and R. Kirchheim, J. Less-Common Metals, 103 (1984) 81.
[4] R. Fromageau and A. Magnouche, Z. Phys. Chem. Neue Folge, 145 (1985) 269.
[5] R. Kirchheim and U. Stolz, J. Non-Cryst. Solids, 70 (1985) 323–341.
[6] A. Szokefalvi-Nagy, S. Filipek and R. Kirchheim, J. Phys. Chem. Solids, 48 (1987) 613.
[7] O. Yoshinari and R. Kirchheim, J. Less-Common Metals, 172–174 (1991) 890.
[8] N. Itoh, W. Xu and K. Haraya, J. Membrane Sci., 66 (1992) 149.
[9] A. Yokoyama and H. Komiyama, H. Inoue, T. Masumoto and H. Kimura, J. Non-Cryst. Solids, 61–62 (1984) 619.
[10] H. Yamashita, M. Yoshikawa, T. Funabiki and S. Yoshida, J. Chem. Soc., Faraday Trans., 1, 81 (1985) 2485.
[11] T. Takahashi and Y. Nishi, N. Otsuji, Kai, T. Masumoto and H. Kimura, Can. J. Chem. Eng., 65 (1987) 274.
[12] H.S. Chen and C.E. Miller, Rev. Sci. Instrum., 41 (1970) 1237.